Distribution of collagen fibril diameter
in the normal skin

Distribution of collagen fibril diameter
in the patient skin

Fig. 4 Distribution of the fibril diameters of the collagen fibers as observed by electron microscopy

Analysis of newly synthesized collagen

To confirm the reduced production of type III collagen in cultured dermal fibroblasts, the collagen synthesis from cultured dermal fibroblasts was analyzed as previously described [5]. Briefly, fibroblast cultures were established by the outgrowth method from skin biopsy specimens, as described previously [3], and the fibroblasts reaching confluence were incubated with DMEM containing 1% FBS and 5 μCi/ml of 2,3-[^{3}H]proline (Amersham) in the presence of 50 μg/ml L-ascorbic acid 2-phosphate for 24 h. Labeled proteins secreted into the culture medium were precipitated by the addition of 5% (final conc.) trichloroacetic acid, and the precipitate was dissolved in 0.05 M acetic acid and digested with pepsin. Then, the labeled proteins were separated by SDS-polyacrylamide gel electrophoresis (5% polyacrylamide gel containing 3.6 M urea) in the presence or absence of 2-mercaptoethanol (which was added for reduction of samples). Radioactive bands were detected by fluorography, and the relative amounts of collagen were quantified by densitometry.

Analysis of sequence of the α1 type III collagen gene (COL3A1)

With regard to analysis of *COL3A1*, the cDNA was analyzed first, followed by analysis of the genomic DNA. Total RNA was extracted from cultured dermal fibroblasts with phenol/guanidium isothiocyanate (Trizol Reagent, Invitrogen), and cDNA was synthesized using the Rever-Tra Ace-α (TOYOBO) Kit. PCR was performed using

primer pairs established to allow the analysis of all the triple-helical sites of *COL3A1* and the cDNA. After confirming the DNA amplification by agarose gel electrophoresis, we conducted direct sequencing using the ABI PRISM 3100 genetic analyzer (ABI Advanced Biotechnologies, Columbia, MD, USA). Genomic DNA was extracted from the blood in accordance with a previously established method [6], and the necessary portion was amplified by PCR and analyzed by sequencing in a similar way to that described above.

Results

Newly synthesized collagen

While the amount of type I collagen produced by the patient's cultured fibroblasts was almost the same as that produced by fibroblasts derived from healthy subjects, the amount of type III collagen produced by the patient's fibroblasts was markedly reduced as compared with that by fibroblasts derived from healthy subjects (Fig. 5); the amount of type III collagen synthesized by the patient's fibroblasts was only 15.0% of that produced by fibroblasts derived from healthy subjects.
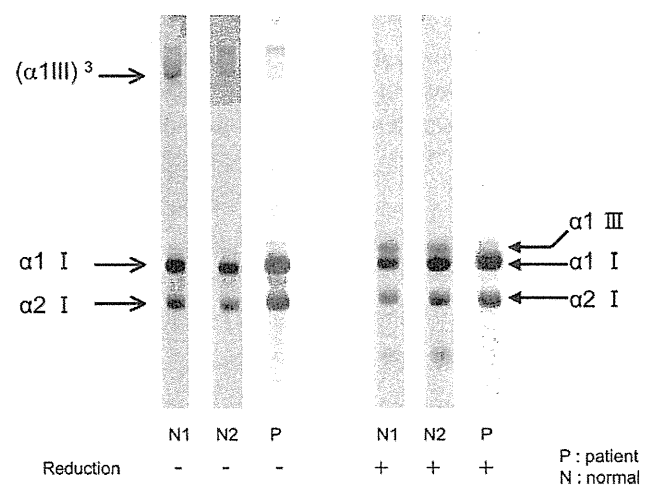

Fig. 5 Fluorograms of sodium dodecylsulphate (SDS)-polyacrylamide gel electrophoresis of collagen molecules obtained from the dermal fibroblast culture medium of the patient (*P*) and an age- and sex-matched normal volunteer (*N*). Fibroblasts were cultured in medium containing ^{3}H-proline for 24 h. After treatment of the collagen samples prepared from the culture medium with 0.1% pepsin, they were separated by SDS/5% polyacrylamide gel electrophoresis in the presence (+ reduction) or absence (− reduction) of 2-mercaptoethanol. Although the patient's fibroblasts produced an equal amount of type I collagen to the normal control fibroblasts, production of type III collagen from the patient fibroblasts was markedly reduced
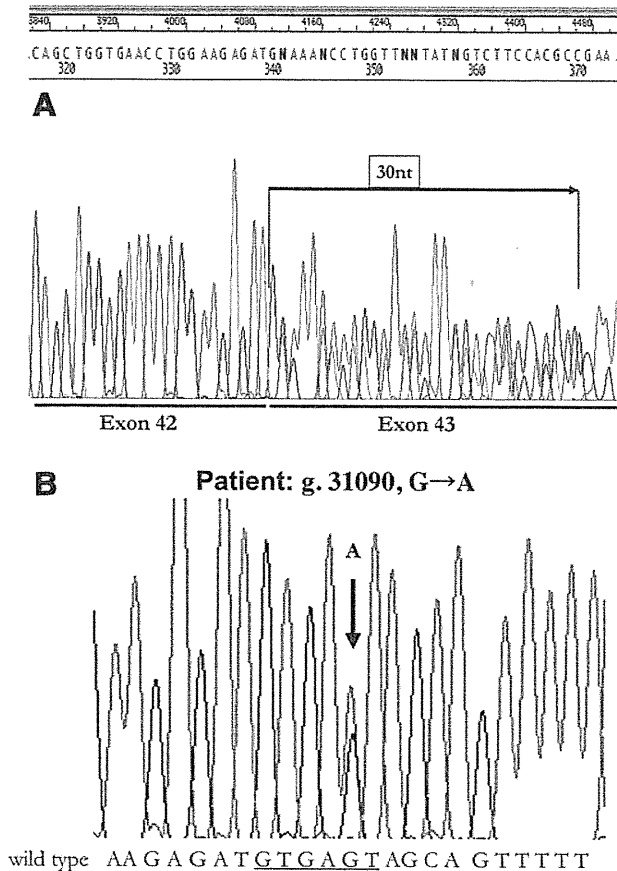
Fig. 6 Search for *COL3A1*. **a** Analysis of the *COL3A1* cDNA, which was synthesized from RNA obtained from the patient's fibroblasts. A part of exon 43 was unreadable. The analysis revealed inclusion of 30 nucleotides (nt) downstream from the tip of intron 42 that contained a G to A mutation of g. 31090 between exon 42 and exon 43 of one allele of the cDNA of *COL3A1*. **b** Analysis of the genomic DNA revealed a mutation of GTGAGT to GTGAAT at donor splice-site +5 of intron 42 (g. 31090 G > A). The donor splice-site is *underlined*

Mutations detected in the COL3A1

The cDNA analysis results revealed inclusion of 30 nt between Exon 42 and Exon 43 of one allele (Fig. 6a). The region near the genomic DNA was amplified by PCR for analysis of the genomic DNA; the result revealed G to A transition at the donor splice-site +5 (g. 31090) of intron 42 (IVS 42 G^{+5} to A) of the *COL3A1* (Fig. 6b). Inclusion of 30 nt of the cDNA was revealed to be 30-nt downstream from the tip of intron 42 which contained the mutation (correspond to 10 amino acids, VNSSFYSTSQ). When the genomic DNA extracted from the patient's parents' blood was analyzed for donor splice-site +5 (g. 31090) mutation of intron 42, heterozygous G to A mutation, the same as that seen in the patient, was recognized in the mother.

Discussion

Our patient exhibited three of the four major diagnostic criteria [1] for the vascular type of EDS, i.e., thin, translucent skin, extensive bruising, and the characteristic facies, and at least four of the nine minor diagnostic criteria, i.e., acrogeria, hypermobility of the small joints, pneumothorax, and a positive family history. Based on these findings, a clinical diagnosis of the typical vascular type of EDS was made. Neither our patient nor her mother had developed any severe complications, including arterial rupture, aneurysm, and/or dissection, gastrointestinal perforation or rupture, or uterine rupture during pregnancy. An aggregated calculation in the US suggested a low incidence of these complications during childhood in patients with the vascular type of EDS, but increases with age. According to the report, complications are recognized for the first time by the age of 20 years in 25% of the patients, and at least 1 complication is recognized by the age of 40 years in at least 80% of the patients [11]. Therefore, rigid follow-up of both the patient and her mother is needed for early detection of possible severe complications in the future.

The vascular type of EDS is caused by abnormality in the synthesis of type III collagen molecules, attributable to heterozygous mutation of the *COL3A1*. In most cases, the mutation is a substitution mutation of glycine at the triple-helical domain, or a splice-site mutation at the junction of the triple-helical exon, the former accounting for about two-thirds of all the mutations reported, and the latter for about one-third of all the cases [10]. In our present patient, a point mutation of G to A at the donor splice-site +5 (g. 31090) of intron 42 (IVS 42 G^{+5} to A) of the *COL3A1* was detected. This was also associated with inclusion of 30 nt downstream from the tip of intron 42 containing this mutation in the cDNA (the mature mRNA). To explain these observations, the following may be considered: there may be a potential donor splice-site 30 nt downstream from the tip of intron 42 in the genomic DNA of the *COL3A1*; in our patient, because the mutation at the donor splice-site of the tip of intron 42 (the original one), a new cryptic donor splice-site (AG/GTAGAA, where "/" denotes the site of cleavage), was recognized, normal cleavage at the terminal of exon 42 did not occur and the cleavage occurred at this site during the splicing, resulting in the production of a mature mRNA containing an additional 30 nt in response to the read-through to a cryptic donor site at 30 nt downstream (Fig. 7).

A similar mutation was reported by Giunta and Steinmann [4]; they reported a mutation at the donor splice-site of intron 42 of the *COL3A1*, which was a point mutation of G^{+5} to C (IVS 42 G^{+5} to C). Also, similar to the observation in our case, they recognized a 30-nt inclusion in the mature mRNA. Schwarze et al. [10] also reported a point mutation

Fig. 7 Schematic representation of a point mutation (IVS 42 $G^{+5} \rightarrow$ A) in *COL3A1*, resulting in inclusion of 30 nucleotides (nt) in the mature mRNA. Exons are represented as *boxes*, and intron sequences are signified by *lower-case letters*. The *underline* in the mRNA indicates a mutation
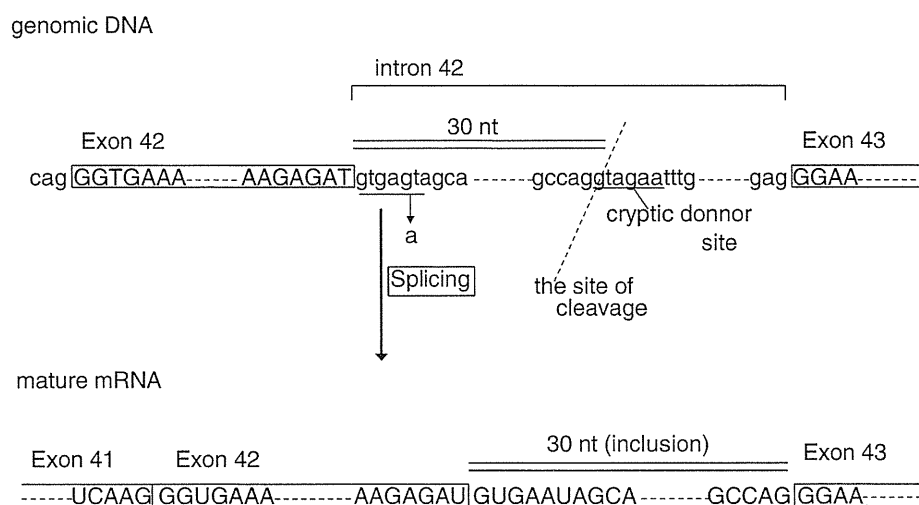
of G^{+1} to A (IVS 42 G^{+1} to A) at the donor splice-site of intron 42 of the *COL3A1* and a 30-nt inclusion in the mature mRNA. To the best of our knowledge, however, there are no other reports, until date, of genetic mutation of the *COL3A1* identical to that confirmed in our case [2]. Type III collagen spirals with the same three α1 (III) chains to form a triple helix (homo-trimer), and the site of the triple helix shows regular amino acid repeats of $(Gly\text{-}X\text{-}Y)_{343}$ [9]. Therefore, in type III collagen, to ensure proper assembly of the alpha homo-trimers, the Gly-Y-Y repeats must not contain skips, and the length of the triple helix should be the same for each α chain [10, 11]. With regard to the inclusion of the 30 nt into the triple-helical domain of the *COL3A1* in our case, 10 amino acids (VNSSFYSTSQ) that were not Gly-X-Y repeats were included into the triple helix of type III collagen, with ensuing failure of formation of the healthy type III collagen molecule and the development of this disease.

Our patient had a history of pneumothorax as a known complication of the disease, but no other severe complications had developed yet. No associations are observed between the type of complication and any specific mutations, according to previous reports [7, 8].

References

1. Beighton P, De Paepe A, Steinmann B, Tsipouras P, Westrup RJ (1998) Ehlers–Danlos syndrome: revised nosology, Villefranche. J Med Genet 77:31–37. doi:10.1002/(SICI)1096-8628(19980428)77:1<31::AID-AJMG8>3.0.CO;2-O

2. Dalgleish R (1998) The human collagen mutation database. Nucleic Acids Res 26:253–255. doi:10.1093/nar/26.1.253

3. Fleischmajer R, Perlish JS, Krieg T, Timple R (1981) Variability in collagen and fibronectin synthesis by scleroderma fibroblasts in primary culture. J Invest Dermatol 76:400–403. doi:10.1111/1523-1747.ep12520933

4. Giunta C, Steinmann B (2000) Characterization of 11 new mutations in COL3A1 of individuals with Ehlers–Danlos syndrome type IV: preliminary comparison of RNase cleavage, EMC and DHPLC assays. Hum Mutat 16:176–177. doi:10.1002/1098-1004(200008)16:2<176::AID-HUMU12>3.0.CO;2-E

5. Hata R, Kurata S, Shinkai H (1988) Existence of malfunctioning pro α2(I) collagen genes in a patient with a pro α2(I)-chain-defective variant of Ehlers–Danlos syndrome. Eur J Biochem 174:231–237. doi:10.1111/j.1432-1033.1988.tb14087.x

6. Hatamochi A, Ono M, Ueki H, Namba M (1991) Regulation of collagen gene expression by transformed human fibroblasts: decreased type I and type III collagen RNA transcription. J Invest Dermatol 96:473–477. doi:10.1111/1523-1747.ep12470171

7. Oderich GS, Pannecton JM, Bower NM, Bower TC, Lindor NM, Cherry KJ Jr, Noel AA, Kalra M, Sullivan T, Gloviczki P (2005) The spectrum, management and clinical outcome of Ehlers–Danlos syndrome type IV: a 30-year experience. J Vasc Surg 42:98–106. doi:10.1016/j.jvs.2005.03.053

8. Pepin M, Schwarze U, Superti-Furga A, Byers PH (2000) Clinical and genetic features of Ehlers–Danlos syndrome type IV, the vascular type. N Engl J Med 342:673–680. doi:10.1056/NEJM200003093421001

9. Pope FM, Narcisi P, Nicholis AC, Germaine D, Pals G, Richards AJ (1996) *COL3A1* mutations cause variable clinical phenotypes including acrogeria and vascular rupture. Br J Dermatol 135:163–181. doi:10.1111/j.1365-2133.1996.tb01143.x

10. Schwarze U, Goldstein JA, Byers PH (1997) Splicing defects in the *COL3A1* gene: marked preference for 5'(donor) splice-site mutations in patient with exon-skipping mutations and Ehlers–Danlos syndrome type IV. Am J Hum Genet 61:1276–1286. doi:10.1086/301641

11. Watanabe A, Kosho T, Wada T, Sakai N, Fujimoto M, Fukushima Y, Shimada T (2007) Genetic aspects of vascular type of Ehlers–Danlos syndrome(vEDS, EDSIV) in Japan. Circ J 71:261–265

INTERNAL MEDICINE

Ehlers-Danlos Syndrome Type IV, Vascular Type, Which Demonstrated a Novel Point Mutation in the COL3A1 Gene

Rinako Sadakata[1], Atsushi Hatamochi[2], Keiji Kodama[1,3], Akiko Kaga[1],
Takefumi Yamaguchi[1], Tomoyuki Soma[1], Yutaka Usui[1], Makoto Nagata[1], Akira Ohtake[4],
Koichi Hagiwara[1] and Minoru Kanazawa[1]

Abstract

Ehlers-Danlos syndrome type IV (EDS type IV), vascular type, an autosomal dominant disorder caused by a mutation of the type III procollagen gene (COL3A1) is the most severe form of EDS and often presents with aortic hemorrhage or organ perforation. This report discusses a male patient with EDS type IV with dyspnea due to hemopneumothorax. He had thin skin and hypermobile joints and was clinically confirmed as having EDS type IV. The diagnosis was genetically confirmed by a mutation c.2528 G>A (p.Gly843Glu) in the COL3A1 gene. The position of the mutation has never been reported.

Key words: Ehlers-Danlos syndrome type IV, collagen type III, mutation, Col3A1

Introduction

Ehlers-Danlos syndrome, type IV (EDS IV: MIM 130050), also known as EDS vascular type, is a rare autosomal dominant disease seen at a frequency of 1:250,000 (1) and is characterized by elastic skin, fragile tissue and fragile arteries that lead to arterial rupture, aortic dissection and gastrointestinal perforation. EDS type IV is caused by a mutation in the COL3A1 gene located on 2q31 that encodes pro-α1 chain of type III collagen (2), and the penetrance of the mutated gene is thought to be 1.0. The mutation causes reduced production or decreased function of the type III collagen, resulting in the signs and symptoms observed in the patients (1, 3).

We present the case of a male patient with EDS type IV which was clinically diagnosed and was genetically confirmed by a mutation c.2528 G>A (p.Gly843Glu) in the COL3A1 gene.

Case Report

A 23-year-old male presented with chest pain and dyspnea. He had a thin nose, thin lips and philtrum, small chin, thin and translucent skin, and hypermobile small joints. Thoracic CT revealed pneumothorax and pleural effusion, and the diagnosis of hemopneumothorax was established by thoracentesis (Fig. 1). He was noted to have clubfoot when he was 6 months old and had epilepsy when he was 7 months old (Fig. 2). Diagnostic criteria and standardized nomenclature for the Ehlers-Danlos syndromes has been suggested (Table 1) (4). The presence of one or more major criteria is necessary to establish clinical diagnosis. The presence of one or more minor criteria contributes to the classification into a subtype. This case fulfilled 2 major criteria; thin, translucent skin and characteristic facial appearance, and 4 minor criteria; hypermobility of small joints, talipes equinovarus (clubfoot), pneumothorax/pneumohemothorax, and positive family history, sudden death in a close relative, and the diagnosis of EDS type IV was established.

[1]Department of Respiratory Medicine, Saitama Medical University, Saitama, [2]Department of Dermatology, School of Medicine, Dokkyo Medical University, Saitama, [3]Department of General Internal Medicine, Saitama Medical University, Saitama and [4]Department of Pediatrics, Saitama Medical University, Saitama
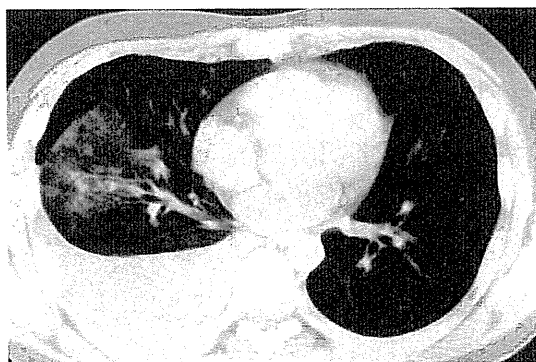
Figure 1. Thoracic CT. Thoracic CT and thoracentesis revealed hemopneumothorax.
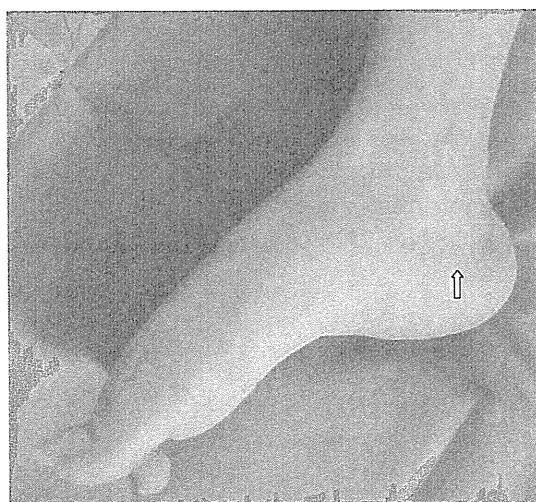

Figure 2. Right foot. The skin was translucent. The wound on his heel was a scar that remained after undergoing surgery for his clubfoot.

A skin biopsy was performed on his upper-arm and the fibroblasts were cultured in order to biochemically and genetically confirm the diagnosis. The fibroblasts were cultured with [^{3}H]proline. Here, most of the radioactive proteins secreted in the culture medium were the type III collages synthesized by the fibroblasts. They were separated by sodium dodecyl-sulfate polyacrylamide gel electrophoresis (SDS-PAGE), imaged by fluorography, and the intensity of each band was measured by a densitometer. The amount of the α1 chain of the type III collagen secreted into the culture medium was only 11% of that of the fibroblasts from sex- and age-matched control (Fig. 3). An investigation of the entire coding sequence of the COL3A1 mRNA revealed a heterozygous point mutation c.2528 G>A in exon 37 that substitutes Gly843 to Glu (Fig. 4). The mutation was then confirmed by the sequence analysis of genomic DNA. Although the mutation was not one of the previously reported mutations, Gly843 is located in one of the Gly-X-Y triplet backbone sequences of the collagen alpha chain where a Gly is required for the trimer of procollagen molecules to form a triple-helix structure. Therefore, the procollagen molecule with a Gly843Glu substitution would have a reduced capacity to form a triple-helix structure and thus re-

Table 1. Diagnostic Criteria of EDS Type IV (4)

i) Major diagnostic criteria.

Thin, translucent skin.

Arterial/intestinal/uterine fragility or rupture.

Extensive bruising.

Characteristic facial appearance.

ii) Minor diagnostic criteria.

Acrogeria.

Hypermobility of small joints.

Tendon and muscle rupture.

Talipes equinovarus (clubfoot).

Early-onset varicose veins.

Arteriovenous, carotid-cavernous sinus fistula.

Pneumothorax/pneumohemothorax.

Gingival recession.

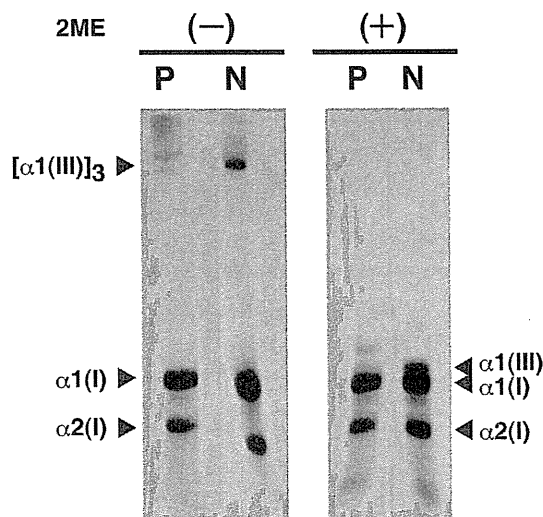Positive family history, sudden death in (a) close relative(s).

Figure 3. Autoradiofluorogram of procollagens secreted from fibroblasts. Cultured fibroblasts were pulse-labelled with [^{3}H]proline in fresh medium and secreted proteins were separated by the sodium dodecyl-sulfate polyacrylamide gel electrophoresis (SDS-PAGE) under normal(-) or reducing(+) conditions (11). α1(I), α2(I) were detected at a similar amount, while the amount of α1(III) was markedly decreased in the patient. P: patient, N: normal control, α1(I), α2(I), and α1(III): α1 chain of type I, α2 chain of type I and 1 chain of type III collagens, respectively, [α1(III)]₃: trimer of the α1 chain of type III collagen, 2ME: 2-mercaptoethanol

c.2528G>A, p.Gly843Glu

Wild type
sequence

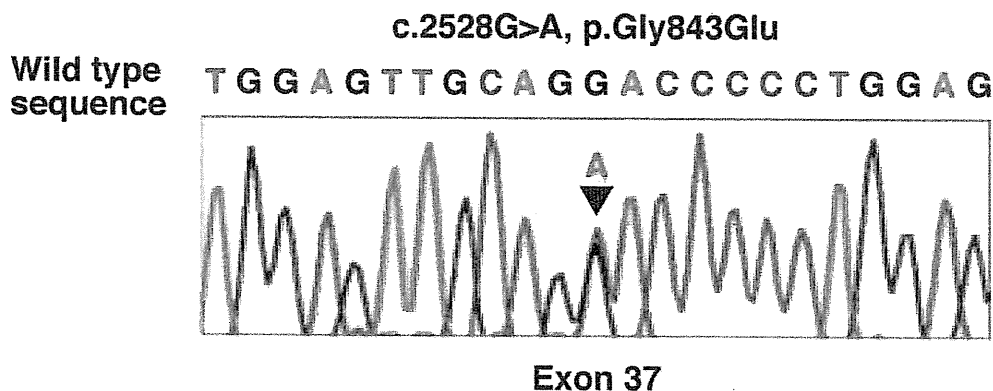T G G A G T T G C A G G A C C C C T G G A G

Exon 37

Figure 4. Heterozygous point mutation in exon 37 of the COL3A1 gene. Fibroblast mRNA was reverse-transcribed and the entire coding sequence of COL3A1 was amplified using the overlapping primers. Direct sequencing of the amplicons revealed c.2,528G>A (p. Gly843Glu) mutation. Wild-type allele and mutant allele were expressed at a similar amount. The presence of mutation was confirmed by the direct sequencing of genomic DNA.

markably reduce the secretion of α1(III) chain of the type III procollagen molecules. We thereby concluded that the mutation was the cause of the EDS type IV in this patient.

During the 2 years that followed the establishment of the diagnosis, he had a total of 6 episodes of pneumothorax and alveolar hemorrhage. A cavity has been formed where once a hematoma was formed. In addition, he developed epileptic seizures, and has been given an anti-epileptic medication.

Discussion

The characteristic clinical signs and symptoms of the EDS type IV have been summarized into the major and the minor diagnostic criteria (1, 4). Over 98% of the patients with EDS type IV have been revealed to have a COL3A1 mutation (1). The patient in the current report is thus demonstrated as a characteristic case with EDS type IV.

Although patients with EDS type IV may have a history of visiting doctors due to minor symptoms such as club-foot or epilepsy, the diagnosis of EDS type IV is often not established until a catastrophic complication appears. The rates of the first symptoms in one study were arterial complications, 46%; gastrointestinal complications, 19%; and other organ complications, 5%. Only 30% of the patients are diagnosed of their disease before a serious complication developed. The median age of the first complication is 23.5 years old, and 12% of them did not survive such a complication (5). EDS type IV is the only EDS that has pneumothorax as one of the diagnostic criteria, and the presence of pneumothorax supports the diagnosis of EDS type IV. Spontaneous pneumothorax has been observed in 16% of the patients with EDS type IV (6, 7).

Surgical treatment is often difficult to perform once a complication develops because of the fragility of vessels (8). Conditions that require surgery include both non-vascular complications such as rupture of bowel, abdominal wall hernias, and miscarriages and vascular complications such as

rupture of aneurysm, and arterial fistula that may lead to compartment syndrome when it occurs within a closed space. The present patient may have future episodes that require surgical treatment and they are a serious concern (9).

Genetic counseling gives potential benefit to the family members of the proband. The penetrance of the gene is close to 1.0, and the disease very often becomes lethal. Taking these factors into consideration, genetic counseling should be considered and deliberately performed.

The mutations of COL3A1 include point mutations in the coding sequence, point mutations in the splicing donor consensus sequence, and deletions (5). Most of the point mutations in the coding sequence changes glycine in one of the Gly-X-Y triplet sequences in the triple-helix domain to another amino acid (5). The substitution of Gly to another amino acid has been found in other hereditary diseases in which causative genes are one of the collagen genes: osteogenesis imperfecta for type I collagen, Alport syndrome for type IV collagen, and dystrophic epidermolysis bullosa for type VII collagen. The substitution of Gly in these collagen molecules is known to destabilize the triple-helix, and thus contributes to the occurrence of pathogenicity (10). The mutated collagen molecule exerts a dominant negative effect to cripple the function of normal collagen molecules produced by the wild-type allele. The c.2528 G>A (p.Gly843Glu) observed in the current patient matched the characteristics of pathogenic mutation.

The current report described a case of EDS type IV that presented a novel mutation in the COL3A1 gene. The information presented here will provide important information for the EDS type IV as well as for the biochemistry of collagen type III.

References

1. Pepin MG BP. Ehlers-danlos syndrome, vascular type. 2006. Available from: http://www.ncbi.nlm.nih.gov/bookshelf/br.fcgi?book=gene&part=eds4

2. Superti-Furga A, Gugler E, Gitzelmann R, Steinmann B. Ehlers-danlos syndrome type iv: A multi-exon deletion in one of the two col3a1 alleles affecting structure, stability, and processing of type iii procollagen. J Biol Chem **263**: 6226-6232, 1988.

3. Callewaert B, Malfait F, Loeys B, De Paepe A. Ehlers-danlos syndromes and marfan syndrome. Best Pract Res Clin Rheumatol **22**: 165-189, 2008.

4. Beighton P, De Paepe A, Steinmann B, Tsipouras P, Wenstrup RJ. Ehlers-danlos syndromes: Revised nosology, villefranche, 1997. Ehlers-danlos national foundation (USA) and ehlers-danlos support group (UK). Am J Med Genet **77**: 31-37, 1998.

5. Pepin M, Schwarze U, Superti-Furga A, Byers PH. Clinical and genetic features of ehlers-danlos syndrome type iv, the vascular type. N Engl J Med **342**: 673-680, 2000.

6. Pepin M, Superti-Furga A, Byers P. Natural history of ehlers-danlos syndrome type iv (eds type iv): Review of 137 cases. Am J Hum Genet **51**: 44, 1992.

7. Oderich GS, Panneton JM, Bower TC, et al. The spectrum, management and clinical outcome of ehlers-danlos syndrome type iv: A 30-year experience. J Vasc Surg **42**: 98-106, 2005.

8. Roseborough GS, Williams GM. Marfan and other connective tissue disorders: Conservative and surgical considerations. Semin Vasc Surg **13**: 272-282, 2000.

9. Ng SC, Muiesan P. Spontaneous liver rupture in ehlers-danlos syndrome type iv. J R Soc Med **98**: 320-322, 2005.

10. Brodsky B, Thiagarajan G, Madhan B, Kar K. Triple-helical peptides: An approach to collagen conformation, stability, and self-association. Biopolymers **89**: 345-353, 2008.

11. Bonadio J, Holbrook KA, Gelinas RE, Jacob J, Byers PH. Altered triple helical structure of type i procollagen in lethal perinatal osteogenesis imperfecta. J Biol Chem **260**: 1734-1742, 1985.

Pleuropulmonary pathology of vascular Ehlers–Danlos syndrome: spontaneous laceration, haematoma and fibrous nodules

Yoshinori Kawabata, Akira Watanabe,[1] Shozaburo Yamaguchi,[2] Masahiro Aoshima,[3] Akira Shiraki,[4] Atushi Hatamochi,[5] Tetsuji Kawamura,[6] Takashi Uchiyama,[7] Atushi Watanabe[8] & Yuh Fukuda[9]

Division of Pathology, Saitama Cardiovascular and Respiratory Centre, Saitama, [1]Division of Control and Treatment of Infectious Diseases, Chiba University Hospital, Chiba, [2]Department of Pulmonary Medicine, Saitama Cardiovascular and Respiratory Centre and [3]Department of Pulmonary Medicine, Sekisinkai Sayama Hospital, Saitama, [4]Department of Respiratory Medicine, Nagoya University Graduate School of Medicine, Nagoya,[5]Department of Dermatology, Dokkyo Medical University, Tochigi, [6]Department of Pulmonary Medicine, National Hospital Organization Himeji Medical Centre, Himeji, [7]Department of Pulmonary Medicine, Double Red Cross Hospital, [8]Division of Clinical Genetics, Nippon Medical School Hospital and [9]Department of Analytic Human Pathology, Nippon Medical School, Tokyo, Japan

Aims: The aim was to clarify the pleuropulmonary pathological findings of vascular Ehlers–Danlos syndrome (vEDS).

Methods and results: Nine patients with confirmed vEDS by means of cell culture and/or molecular biological studies who had undergone surgical lung biopsy (SLB), lobectomy or autopsy were studied. Six patients were male and three were female with a mean age of 23.2 years. Histological features were as follows: (i) the main pulmonary lesions related to fragility and spontaneous laceration, these being haematomas in seven, acute haemorrhage in nine, fibrous nodule in eight, with ossification or bone marrow formation in six; vascular disruption in five; intraluminal haemosiderosis in nine; interstitial haemosiderosis in seven, with iron deposition in the alveolar wall and/or vessel wall in five and foreign body reaction in two; emphysematous changes in eight; and bleb formation in two; (ii) secondary iatrogenic pleuropulmonary injuries during SLB or lobectomy comprised pleural laceration in seven of 10 and lung laceration in eight of 10 specimens.

Conclusions: Spontaneous laceration of lung tissue is an essential feature and is followed by haematoma and possible fibrous nodule formation.

Keywords: haematoma, haemosiderosis, laceration, lung, pseudotumour

Abbreviations: EVG, Elastica–van-Gieson; SLB, surgical lung biopsy; vEDS, vascular Ehlers–Danlos syndrome

Introduction

Vascular Ehlers–Danlos syndrome (vEDS),[1,2] formerly known as Ehlers–Danlos syndrome type IV,[3] is a rare autosomal-dominant hereditary disease. The disorder is caused by a mutation within the *COL 3A1* gene, which encodes the chains of type III procollagen homotrimer.[4,5] This mutation causes abnormalities of the structure, synthesis and secretion of type III procollagen, leads to tissue fragility, and induces many severe

Address for correspondence: Y Kawabata, Division of Pathology, Saitama Cardiovascular and Respiratory Centre, 1696, Itai, Kumagaya, Saitama, Japan 360-1005. e-mail: k369900q@pref.saitama.lg.jp

clinical symptoms, mainly due to vascular and organ rupture.[2] The pathological features of pulmonary and pleural lesions of vEDS were first reported by Corrin *et al.*,[6] but have not been thoroughly elucidated. The purpose of this study was to document the features of pleuropulmonary pathology in patients confirmed to have vEDS.

Methods and materials

Slides were reviewed from nine patients confirmed to have vEDS by means of culture of skin fibroblasts (confirmation of abnormal type III procollagen production) and/or molecular biological analysis (confirmation of the *COL3A1* gene mutation)[2,7] with the consent of the patient or family (Table 1). Four cases (cases 1, 3, 5 and 8) have been reported previously.[8-11] Six patients had undergone surgical lung biopsy (SLB) for abnormal pulmonary shadows or for pneumothorax (twice in one patient), two patients underwent lobectomy (twice in one patient) for haemothorax or haemoptysis, and one patient had undergone autopsy. Only one patient (case 6) was diagnosed with vEDS prior to histopathological examination. In the remainder, pathological findings such as pulmonary haematoma and fibrous nodule led to a suspected diagnosis of vEDS, and patients then underwent definitive procedures. The number of slides examined was 1–41 with a median of 5 (Table 1). Haematoxylin and eosin and Elastica–van-Gieson (EVG) staining was undertaken on all cases, and iron staining was performed as appropriate.

Table 1. Clinical and pleuropulmonary pathological features of each case

Case	1	2	3	4	5	6	7	8–1	8–2	9–1	9–2
Method	SLB	Lo.	SLB	SLB	Aut	SLB	SLB	SLB	SLB	Lo.	Lo.
No. of slides	1	41	11	1	5	2	3	2	5	10	17
Age	16	32	20	22	43	17	26	17	18	16	19
Sex	W	M	M	W	M	W	M	M		M	
Pleural fibrosis/adhesion	+	+	+	+	+	+	−	−	−	+	+
Haematomas of lung	−	++	+	−	+	−	+	+	−	++	++
Acute haemorrhage	+	++	+	−	++	−	++	+	+	++	++
Fibrous nodules	++	+	++	+++	++	−	+	+	−	−	++
With ossification	+	+	−	++	++	/	−	+	/	/	+
Intraluminal organization	−	+	+	−	−	−	++	−	−	−	+
Haemosiderosis, lumina	++	++	++	−	++	+	++	++	−	+	++
Haemosiderosis, walls	+	−	+	−	++	+	+	+	−	−	++
Iron deposition	−	−	+	−	−	+	+	+	−	−	+
Foreign body reaction	−	−	+	−	−	−	−	−	−	−	+
Vascular disruption	−	+	+	−	−	−	+	+	−	−	+
Emphysema	−	+	+	+	++	+	+	−	−	+	+
Bleb	−	−	−	−	−	+	−	−	−	+	−
Iatrogenic pleural disruption	+	+	+	−	/	−	+	+	−	+	+
Iatrogenic lung disruption	+	+	+	−	/	−	+	+	+	+	+

SLB, surgical lung biopsy; Lo., lobectomy; Aut, autopsy; W, women; M, men.

Histological features were assessed as follows:

1 Essential pleuropulmonary lesions related to fragility or weakness of pleuropulmonary tissues and subsequent lesions. Such lesions included pleural adhesion or fibrosis; acute and organizing haematomas of the lung (+, <30 mm in diameter; ++, >30 mm in diameter); acute haemorrhage (+, <10% of slides; ++, >10% of slides); fibrous nodules, including well-defined nodules and irregularly shaped scar tissue (+, <3/1 slide; ++, <10/1 slide; +++, >10/1 slide); ossification in the fibrous nodules (same criteria as above); intraluminal fibroblastic organization (same criteria as above); haemosiderosis in the alveolar lumens (+, patchy; ++, diffuse or massive) and walls (+, patchy; ++, diffuse); deposition of iron in the elastic tissue and/or alveolar basement membrane; foreign body reaction or endogenous pneumoconiosis, vascular disruption of elastic and muscular pulmonary arteries and veins; various types of emphysematous changes, including bullae and paracicatrical emphysema (+, <10% of slides; ++, >10% of slides); and intrapleural cysts or blebs.

2 Secondary iatrogenic pleuropulmonary injury during SLB or lobectomy, including laceration or disruption of the pleura and the lung at the time of SLB or lobectomy. Iatrogenic pleuropulmonary lacerations were confirmed (i) by the surgeon during the procedure and (ii) by no tissue reaction except for occasional haemorrhage to slit-like laceration on histology.

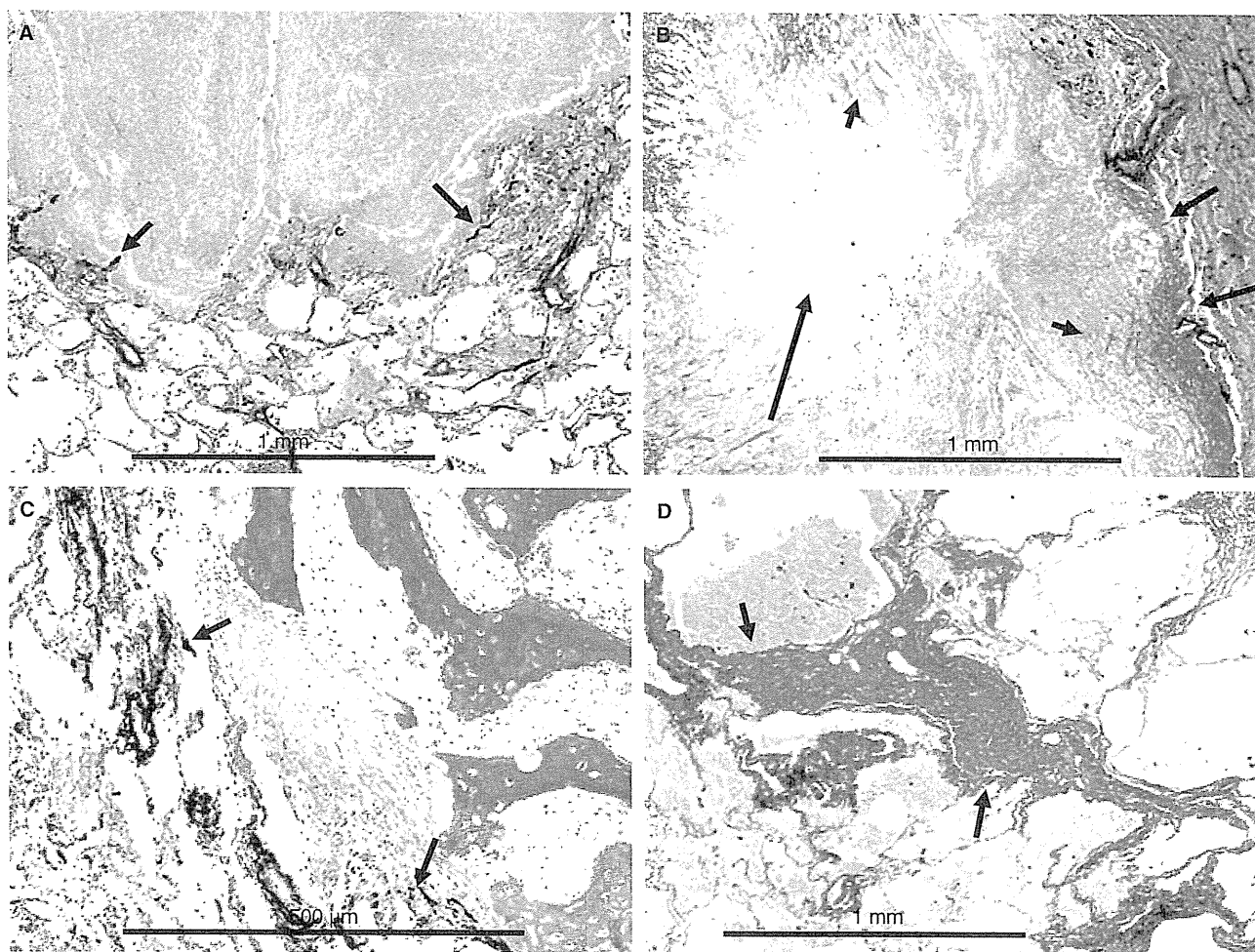This study was approved by the ethics committee of each hospital.

Figure 1. A, An acute pulmonary haematoma shows compression without involvement of lung tissue (arrows). Bar = 1 mm. Elastica–van-Gieson (EVG) staining. B, An organizing pulmonary haematoma shows cavitation of the blood clot (long arrow). Encapsulating fibrosis is seen on the right side (middle arrow), and extension of collagen fibre from the fibrous capsule into the haematoma is also present (short arrow). Bar = 1 mm. (EVG.) C, An organizing fibrous nodule with ossification shows well-defined organization with metaplastic ossification within the fibrosis. The arrow indicates compressed lung tissue. Bar = 500 μm. (EVG.) D, An irregularly shaped scar tissue (arrow) is composed of a thick bundle of mature collagen without involvement of alveolar wall. Bar = 1 mm. (EVG.)

Results

Six patients were male and three female. Age at the time of first pathological examination ranged from 16 to 43 years (mean 23.2 years) (Table 1).

1 Essential pleuropulmonary lesions related to fragility or weakness of pleuropulmonary tissues and subsequent lesions. Focal or diffuse pleural fibrosis and/or adhesion was seen in seven and healed lacerations in two (cases 1 and 9 presented with haemopneumothorax clinically) of 11 specimens. Haematoma was seen in seven specimens (+, $n = 4$; ++, $n = 3$) and acute haemorrhage, including surrounding acute haematoma, was seen in nine procedures (+, $n = 4$; ++,

$n = 5$). The largest haematoma was 50 mm in diameter obtained at lobectomy. Acute haematoma contained no lung tissue within the area of haemorrhage, but compressed the surrounding lung (Figure 1A). Organizing and organized haematoma frequently showed cavity formation (Figure 1B, long arrow) and/or collagen deposition within the haematoma continuous with its wall (Figure 1B, short arrow) and also lacked lung tissue within the haematoma. Fibrous nodules were seen in eight specimens (+, $n = 3$; ++, $n = 4$; and +++, $n = 1$) and ossification or bone marrow formation in fibrous nodule (Figure 1C) was seen in six of 11 specimens (+, $n = 4$; ++, $n = 2$). Some fibrous nodules were irregularly shaped, stellate
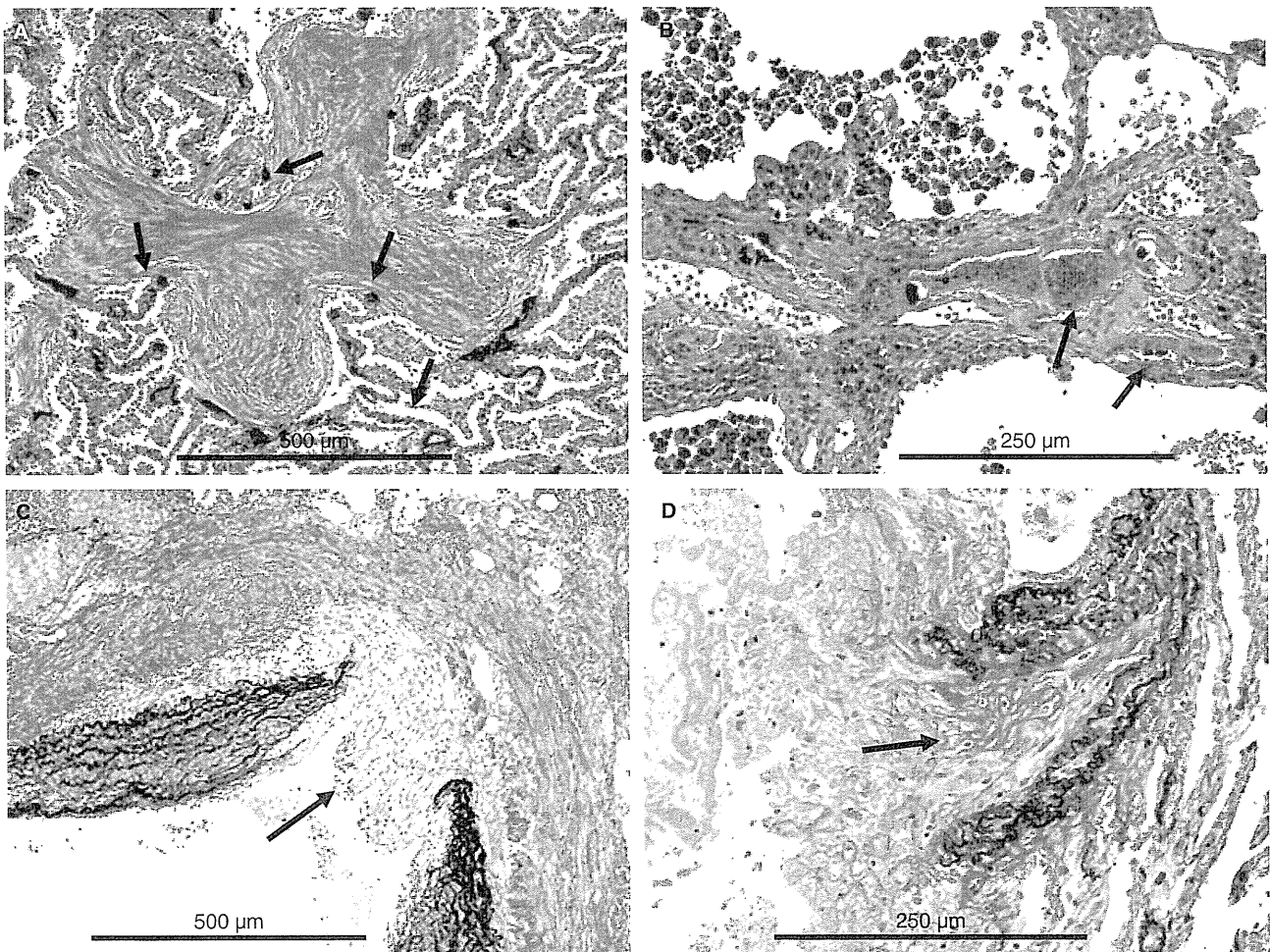

Figure 2. **A**, A bud of organizing pneumonia is located in the alveoli and alveolar sac with preserved lung tissue. Arrows indicate alveolar wall. Bar = 500 μm [Elastica–van-Gieson (EVG)]. **B**, Haemosiderosis. Diffuse and massive haemosiderosis is seen in the alveoli (++) and interstitium (++) and is associated with foreign-body giant cells (arrow). Bar = 250 μm (H&E). **C**, Partial disruption of artery. A portion of the elastic pulmonary artery is disrupted and associated with repair by granulation tissue (arrow). Periarterial connective tissue is not disrupted. Bar = 500 μm (EVG). **D**, Disruption of artery and haematoma. An intermediate-type pulmonary artery shows complete disruption and is associated with fibrous repair (arrow). This artery is located in the fibrous capsule of an organizing haematoma (left side). Arterial rupture with haematoma formation was suspected but not confirmed. Bar = 250 μm (EVG).

(Figure 1D), whereas others showed well-defined, smooth margins. Most of these nodules lacked incorporated lung tissue, rather they compressed surrounding lung tissue confirmed by EVG staining (Figure 1C,D). Interlobular septal location of fibrous nodules was sometimes noted.

Intraluminal organization, i.e. focal organizing pneumonia with preserved lung structure (Figure 2A), was seen in four (+, $n = 3$; ++, $n = 1$) of 11 specimens. Intraluminal haemosiderosis was seen in nine (+, $n = 2$; ++, $n = 7$) and interstitial haemosiderosis in seven (+, $n = 5$; ++, $n = 2$) of 11 specimens. The location of haemosiderosis varied and was not solely around organizing or organized haematomas or fibrous nodules. Related to interstitial haemosiderosis, iron deposition in alveolar and/or vessel walls was seen in five specimens and was associated with a foreign body reaction (endogenous pneumoconiosis, Figure 2B) to degenerate elastic tissue or basement membrane in two specimens. Vascular disruption was seen in five of 11 specimens, but only a small portion of the vessel walls were disrupted (Figure 2C), except for one muscular artery that showed extensive disruption and evidence of repair, which was located in the wall of the organizing haematoma (Figure 2D). The number of disrupted vessels was one per examined slide, except for one case, which had two vessels. Various types of emphysematous change (centrilobular emphysema, paraseptal emphysema/bulla, paracicatrical emphysema and emphysema of undetermined typed, Figure 3A,B) were seen in eight (+, $n = 7$; ++, $n = 1$), and blebs were seen in two of 11 specimens. Among patients with SLBs (mean age 19 years), emphysema was noted in four of seven.
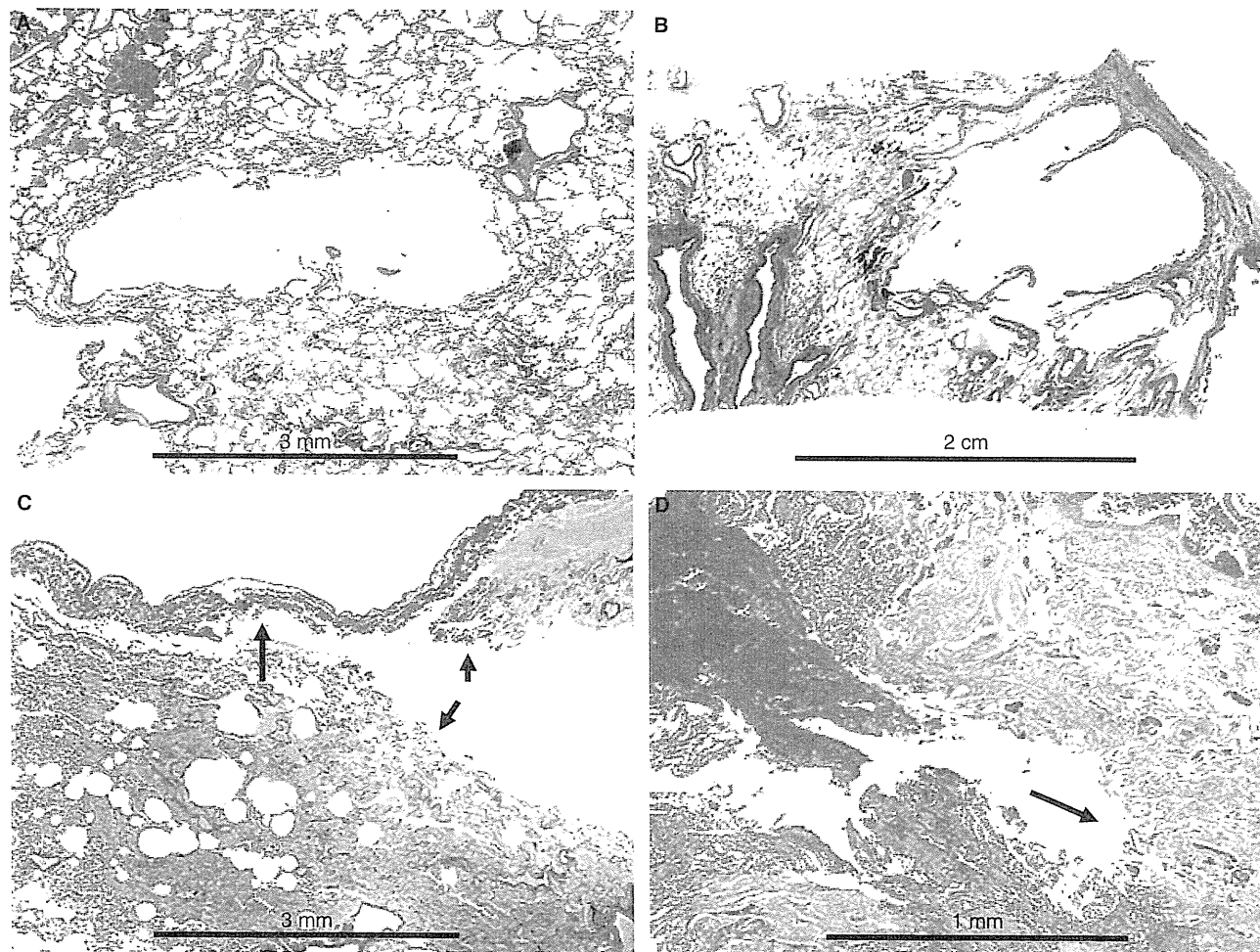

Figure 3. A, Emphysema showing centrilobular distribution. Bar = 3 mm (H&E). B, Paraseptal-type emphysema/bullous emphysema may also be present. Bar = 2 mm (H&E). C, On surgical lung biopsy in this case, the pleura shows laceration (long arrow), and the lung also shows laceration (between short arrows). Bar = 3 mm (Elastica–van-Gieson). D, Lung tissue shows laceration (arrow) with bleeding (left side). Bar = 1 mm (H&E).

Patient 9 underwent two lobectomies (with a 3-year interval) and showed obvious progression of lesions: new appearance of fibrous nodules with ossification, increased degree of intraluminal haemosiderosis, and new appearance of interstitial haemosiderosis with iron deposition and foreign body reaction, although they occurred in different lower lobes.

2 Secondary iatrogenic pleuropulmonary injury during SLB or lobectomy. Pleural laceration (Figure 3C, long arrow) was seen on pathological examination in seven of 10 procedures at SLB or lobectomy, and lung laceration in eight of 10 procedures. Occasionally blood was present within the lacerated lung (Figure 3D).

Discussion

We found haematomas in seven specimens, fibrous nodules in eight, vascular disruption in five, intraluminal haemosiderosis in nine, interstitial haemosiderosis in seven and emphysematous changes in eight of 11, as spontaneous events.

As a pleural complication of vEDS, haemopneumothorax has been reported as a major pleural complication,[9,12,13] but we found only two healed lacerations of the pleura. Intrapulmonary haematoma was more frequently seen, with no lung tissue in the haematoma, only surrounding compressed lung tissue, similar to the findings seen with iatrogenic laceration during the surgical procedure with subsequent bleeding in the lacerated area. Furthermore, because many organizing haematomas showed extension of fibrosis into the haematoma, we speculate that these haematomas shrink and finally become fibrous nodules. The presence of a cavity or cyst on high-resolution computed tomography with subsequent shrinkage has been reported,[12-15] and Herman *et al.*[13] have speculated they are caused by spontaneous rupture; we feel these events might represent haematoma with cavitation and shrinkage, and our data support the speculation of Herman *et al.* Corrin *et al.*[6] speculated that spontaneous tearing may be a cause of pulmonary cyst formation in patients with vEDS.

Fibrous nodules were also seen frequently, most of which did not involve alveolar tissue. We speculate that these nodules without lung tissue might have resulted from small haematomas. Corrin *et al.*[6] have speculated that these fibrous pseudotumours result from tears of lung tissue, and our data are entirely consistent with this hypothesis. Organizing pneumonia was seen in four procedures. We suspect a small injury to the alveolar wall might cause intraluminal exudation and organizing pneumonia. If organizing pneumonia does not resolve, it might be the source of more

established fibrous nodules. However, a few fibrous nodules in our series did involve alveolar tissue; we speculate that these may be related to more severe localized damage.

Vascular disruption was seen in five of 11 specimens, but only a portion of a vessel and only one vessel per slide was observed except for one case. We believe that vascular disruption in the lung is usually not a significant event, perhaps because the pulmonary circulation is a low-pressure system. However, fatal haemoptysis and massive pulmonary haemorrhage due to vascular disruption have been reported.[16]

Haemosiderosis is also a commonly seen feature of vEDS, probably due to vascular disruption. However, we believe alveolar capillary haemorrhage may be an additional if not primary cause of haemosiderosis, rather than localized tears in larger vessels, as there was random distribution of both intraluminal and interstitial haemosiderosis in seven of 11 specimens.

The presence of emphysema has already been reported.[6,15] In our series, various types of emphysema were seen. In particular, SLB showed emphysema in four of seven cases. We speculate that fragility of the alveolar wall, which contains type III collagen, additionally causes other pathologies related to parenchymal and pleural damage, such as interstitial emphysema and bleb formation.

A proposed relationship between the lesions discussed above is shown in Figure 4. We believe spontaneous laceration of lung tissue is the key pathological feature. Following laceration, bleeding from disrupted alveolar walls and pulmonary vasculature makes the
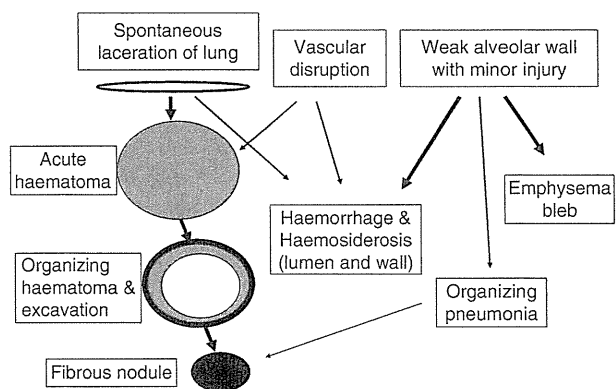
Figure 4. Relationship of each lung lesion in vascular Ehlers–Danlos syndrome. Following spontaneous laceration of lung, acute haematoma formation, organization of haematoma and excavation, finally a fibrous nodule is formed. Vascular disruption might be another source of acute haematoma and haemosiderosis. Following minor spontaneous injury to the alveolar wall, haemorrhage and haemosiderosis, luminal exudation and organization, and tissue destruction (emphysema and bleb) follow.

mechanism of haematoma formation easy to understand, the haematoma space lacking lung tissue as in iatrogenic disruption of lung tissue during SLB. Subsequent events are the organization around haematoma, cavity formation, and fibrosis extending into the haematoma. With shrinkage due to fibrosis, the haematoma finally becomes a small, fibrous nodule. Because haemosiderosis is not specific but is an important component of vEDS, we speculate that alveolar capillary haemorrhage is an additional source as well as disruption of large vessels. We also suspect that haemorrhage, luminal exudation, and organization and tissue destruction might take place following minor spontaneous injury to the alveolar wall.

We also found secondary iatrogenic pleuropulmonary injuries during SLB or lobectomy that comprised pleural laceration in seven and lung laceration in eight of 10 specimens, which may be relevant when planning surgical procedures for suspected cases.

Acknowledgements

References

1. Beighton P, De Paepe A, Steinmann B, Tsipouras P, Wenstrup RJ. Ehlers–Danlos syndromes: revised nosology, Villefranche, 1997. Ehlers–Danlos National Foundation (USA) and Ehlers-Danlos Support Group (UK). *Am. J. Med. Genet.* 1998; **77**; 31–37.
2. Pepin M, Schwarze U, Superti-Furga A, Byers PH. Clinical and genetic features of Ehlers–Danlos syndrome type IV, the vascular? type. *N. Engl. J. Med.* 2000; **342**; 673–680.
3. Beighton P, de Paepe A, Danks D *et al.* International nosology of heritable disorders of connective tissue, Berlin, 1986. *Am. J. Med. Genet.* 1988; **29**; 581–594.
4. Lloyd J, Narcisi P, Richards A, Pope FM. A T + 6 to C + 6 mutation in the donor splice site of COL3A1 IVS7 causes exon skipping and results in Ehlers–Danlos syndrome type IV. *J. Med. Genet.* 1993; **30**; 376–380.
5. Milewicz DM, Witz AM, Smith AC, Manchester DK, Waldstein G, Byers PH. Parental somatic and germ-line mosaicism for a multiexon deletion with unusual endpoints in a type III collagen (COL3A1) allele produces Ehlers–Danlos syndrome type IV in the heterozygous offspring. *Am. J. Hum. Genet.* 1993; **53**; 62–70.
6. Corrin B, Simpson CG, Fisher C. Fibrous pseudotumours, and cyst formation in the lungs in Ehlers–Danlos syndrome. *Histopathology* 1990; **17**; 478–479.
7. Watanabe A, Kosho T, Wada T *et al.* Genetic aspects of the vascular? type of Ehlers–Danlos syndrome (vEDS, EDSIV) in Japan. *Circ. J.* 2007; **71**; 261–265.
8. Nishiyama Y, Nejima J, Watanabe A *et al.* Ehlers–Danlos syndrome type IV with a unique point mutation in COL3A1 and familial? phenotype of myocardial infarction without organic coronary stenosis. *J. Intern. Med.* 2001; **249**; 103–108.
9. Watanabe A, Kawabata Y, Okada O *et al.* Ehlers–Danlos syndrome type IV with few extrathoracic findings: a newly recognized point mutation in the COL3A1 gene. *Eur. Respir. J.* 2002; **19**; 195–198.
10. Ishiguro T, Takayanagi N, Matsushima H *et al.* Ehlers–Danlos syndrome with recurrent spontaneous pneumothoraces and cavitary lesion on chest X-ray as the initial complications. A case report. *Intern. Med.* 2009; **48**; 717–722.
11. Matsushita A, Takayanagi N, Tishiguro T *et al.* A case of Ehlers–Danlos syndrome suspected from pulmonary hematoma due to disruption of the lung. (Japanese with English abstract) *Nihon Kokyuki Gakkai Zasshi* 2009; **47**; 704–710.
12. Murray RA, Poulton TB, Saltarelli MG *et al.* Rare pulmonary manifestation of Ehlers–Danlos syndrome. *J. Thorac. Imaging* 1995; **10**; 138–141.
13. Herman TE, McAlister WH. Cavitary pulmonary lesions in type IV Ehlers–Danlos syndrome. *Pediatr. Radiol.* 1994; **24**; 263–265.
14. Dowton SB, Pincott S, Demmer L. Respiratory complications of Ehlers–Danlos syndrome type IV. *Clin. Genet.* 1996; **50**; 510–514.
15. Sareli AE, Janssen WJ, Sterman D, Saint S, Pyeritz RE. Clinical problem-solving What's the connection?. *N. Engl. J. Med.* 2008; **358**; 626–632.
16. Yost BA, Vogelsang JP, Lie JT. Fatal hemoptysis in Ehlers–Danlos syndrome. Old malady with a new curse. *Chest* 1995; **107**; 1465–1467.

Case Report

Too friable to treat?

Kensuke Kimura, Miho Sakai-Kimura, Ryuichi Takahashi, Atsushi Watanabe, Makio Mukai, Shigetaka Noma, Keiichi Fukuda

Lancet 2010; 375: 1578

Department of Regenerative Medicine and Advanced Cardiac Therapeutics, Keio University School of Medicine (K Kimura MD, Prof K Fukuda MD), Division of Diagnostic Pathology, Keio University Hospital (M Mukai MD), Shinjuku-ku, Tokyo, Japan; Department of Rheumatology and Infectious Diseases, Kitasato University School of Medicine, Sagamihara, Kanagawa, Japan (M Sakai-Kimura MD); Department of Cardiovascular Surgery (R Takahashi MD) and Department of Cardiology (S Noma MD), Saiseikai Utsunomiya Hospital, Utsunomiya, Tochigi, Japan; and Division of Clinical Genetics, Nippon Medical School Hospital, Bunkyo-ku, Tokyo, Japan (A Watanabe MD).

Correspondence to:
Dr Kensuke Kimura, Department of Regenerative Medicine and Advanced Cardiac Therapeutics, Keio University School of Medicine, 35 Shinanomachi, Shinjuku-ku, Tokyo 160-8582, Japan
kimuken@cpnet.med.keio.ac.jp

In February, 2002, a 24-year-old woman was admitted to our hospital with severe chest pain. The pain developed when she was cycling. Nitrates administrated by her general practitioner effectively improved both the symptoms and the ST-segment elevations in leads V1 to V5 of the electrocardiogram. In view of probable acute coronary syndrome, she was admitted to our hospital and underwent immediate cardiac catheterisation. Although coronary angiography showed an intact right coronary artery (RCA) and left circumflex coronary artery (LCX), diffuse stenosis without a radiolucent flap was detected from the mid to distal segments of the left anterior descending coronary artery (LAD) (figure A). Despite spontaneous reperfused LAD flow, the narrowed lumen was unresponsive to either isosorbide dinitrate or nicorandil infusion. The left-ventricular ejection fraction was 48%, and maximum serum concentrations of creatine kinase and the MB isozyme were 2069 IU/L and 186 µg/L respectively (normal range 32–180 IU/L and <5·0 µg/L) 6 h after the onset of chest pain. The patient had no family history of cardiovascular disease, atherosclerotic risk factors, predisposition for hypercoagulability (lupus anticoagulant-negative; anti-cardiolipin-β2-GP1 antibody <1·2 IU/mL; no use of oral contraceptives), or indications of inflammatory disease (antinuclear antibody <×40; antineutrophil cytoplasmic antibodies negative). Refractory vascular spasm or spontaneous coronary artery dissection was therefore considered as the diagnosis. We started treatment with aspirin, an angiotensin receptor blocker, diltiazem, and heparin.

Her clinical course was stable and coronary angiography was done to follow up the LAD lesion 26 days after onset. Surprisingly, despite the spontaneously repaired LAD, both the RCA and LCX had intimal tears that were accompanied by luminal irregularities, indicating several coronary dissections (figure B). The procedure was momentarily paused while treatment options were discussed; at this point, the patient developed chest pain. Coronary angiography showed that the dissection had extended from the LCX to the LAD via the left main trunk, and that the LAD was totally occluded in its proximal segment (figure C). Emergency aorto-coronary artery bypass graft surgery using saphenous vein grafts was done. Histopathological examination of the excised aorta showed disorganised media with fragmented elastic fibres, indicating friable vessels. Soon after the patient was discharged, her 21-year-old brother suffered a gastrointestinal rupture and was diagnosed with vascular-type Ehlers-Danlos syndrome. Eventually our patient was shown to have the same mutation as her brother—Gly220Trp in the (Gly-X-Y)n repeat of the triple-helical domain of type III procollagen (COL3A1).[1] Subsequently, the patient's aunt was also suspected of having vascular-type Ehlers-Danlos syndrome. When seen in December, 2009, the patient was doing well.

Vascular-type Ehlers-Danlos syndrome is an autosomal dominant connective tissue disorder caused by abnormal type III collagen, which is the result of mutations in the COL3A1 gene. Because type III collagen is a major component of blood vessels, viscera, and the uterus, affected patients frequently suffer life-threatening ruptures of the bowel and arteries.[2] Although vascular-type Ehlers-Danlos syndrome is difficult to diagnose in a patient who does not have any of the associated physical features, clinicians should consider the possibility of the syndrome when multiple vascular dissections are present, especially in young patients. Of note, angiography can damage the delicate vessels.[3] The friability of the vessels and associated complications have received much attention in surgical publications.[4] However, the optimum treatment for patients with vascular-type Ehlers-Danlos syndrome remains unclear.

References
1 Watanabe A, Kosho T, Wada T, et al. Genetic aspects of the vascular type of Ehlers-Danlos syndrome (vascular-type Ehlers-Danlos syndrome, EDS IV) in Japan. Circ J 2007; 71: 261–65.
2 Pepin M, Schwarze U, Superti-Furga A, Byers PH. Clinical and genetic features of Ehlers-Danlos syndrome type IV, the vascular type. N Engl J Med 2000; 342: 673–80.
3 Fann JI, Dalman RL, Harris JE Jr. Genetic and metabolic causes of arterial disease. Ann Vasc Surg 1993; 7: 530–604.
4 Lauwers G, Nevelsteen A, Daenen G, et al. Ehlers-Danlos syndrome Type IV: a heterogenous disease. Ann Vasc Surg 1997; 11: 178–82.
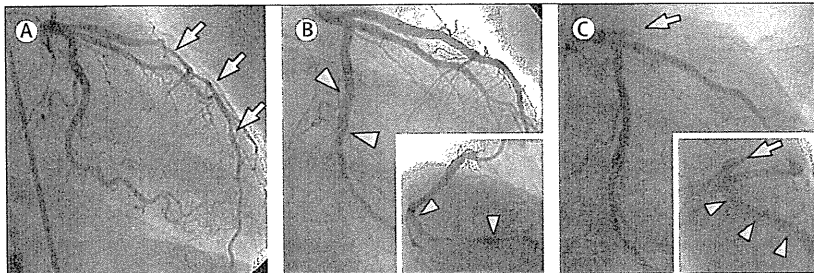
Figure: Angiography
(A) LAD showing diffuse stenosis (arrows) on admission. (B) Follow-up 26 days later shows tearing of the RCA (inset) and LCX (main). (C) After the development of chest pain, the dissection of the LCX has extended to the left main stem (inset, arrow heads) and the LAD is totally occluded (arrow).

A novel mutation screening system for Ehlers-Danlos Syndrome, vascular type by high-resolution melting curve analysis in combination with small amplicon genotyping using genomic DNA

Banyar Than Naing [a], Atsushi Watanabe [a,b,*], Takashi Shimada [a,b]

[a] Department of Biochemistry and Molecular Biology, Nippon Medical School, Tokyo, Japan
[b] Division of Clinical Genetics, Nippon Medical School Hospital, Tokyo, Japan

ARTICLE INFO

ABSTRACT

Ehlers-Danlos syndrome, vascular type (vEDS) (MIM #130050) is an autosomal dominant disorder caused by type III procollagen gene (COL3A1) mutations. Most COL3A1 mutations are detected by using total RNA from patient-derived fibroblasts, which requires an invasive skin biopsy. High-resolution melting curve analysis (hrMCA) has recently been developed as a post-PCR mutation scanning method which enables simple, rapid, cost-effective, and highly sensitive mutation screening of large genes. We established a hrMCA method to screen for COL3A1 mutations using genomic DNA. PCR primers pairs for COL3A1 (52 amplicons) were designed to cover all coding regions of the 52 exons, including the splicing sites. We used 15 DNA samples (8 validation samples and 7 samples of clinically suspected vEDS patients) in this study. The eight known COL3A1 mutations in validation samples were all successfully detected by the hrMCA. In addition, we identified five novel COL3A1 mutations, including one deletion (c.2187delA) and one nonsense mutation (c.2992C>T) that could not be determined by the conventional total RNA method. Furthermore, we established a small amplicon genotyping (SAG) method for detecting three high frequency coding-region SNPs (rs1800255:G>A, rs1801184:T>C, and rs2271683:A>G) in COL3A1 to differentiate mutations before sequencing. The use of hrMCA in combination with SAG from genomic DNA enables rapid detection of COL3A1 mutations with high efficiency and specificity. A better understanding of the genotype–phenotype correlation in COL3A1 using this method will lead to improve in diagnosis and treatment.

1. Introduction

Ehlers-Danlos syndrome, vascular type (vEDS), formerly called type IV EDS (MIM #130050) [1,2], is an autosomal dominant disorder caused by heterogeneous mutations of the gene encoding type III procollagen (COL3A1: MIM #120180) [3]. Its main clinical features are rupture of blood vessels or internal organs such as the uterus and bowel [4,5]. In the management of aneurysms, it is important to distinguish patients with vEDS due to a COL3A1 mutation from other aneurysm syndromes with FBN1 or TGFBR mutations, because tissue friability is different in these syndromes [6]. Since COL3A1 is composed of 52 exons, most COL3A1 mutations

have been detected using a reverse transcriptase PCR (RT-PCR) direct-sequencing method with total RNA extracted from patient fibroblasts, which involves an invasive skin biopsy and cell culture [5]. Therefore, we considered an alternative rapid screening method to detect COL3A1 mutations from genomic DNA.

Most mutation screening methods such as single-strand conformational polymorphism analysis [7], and denaturing high-performance liquid chromatography [8] require post-PCR manipulations, and are time consuming. A new mutation screening system termed "high-resolution melting curve analysis" (hrMCA) has recently been developed for rapid scanning of sequence variants [9–11]. The hrMCA is a closed-tube method that requires only one PCR reaction with fluorescence dye and melting analysis. Because of its ease of use, simplicity, flexibility, low cost, nondestructive nature, and high sensitivity (98%) and specificity (99.4%) [12], hrMCA is quickly becoming the tool of choice for mutation screening, especially of large genes [13].

In this study, we evaluated the hrMCA method using genomic DNA to screen the entire coding region of COL3A1. In addition, we applied detection of high frequency coding-region SNPs in

---

COL3A1 before sequencing, which are difficult to differentiate from mutations by hrMCA.

2. Materials and methods

2.1. Samples

We used 15 genomic DNA samples (8 validation samples with known COL3A1 mutations to validate the hrMCA, and 7 clinically suspected Japanese vEDS patients) in this study. Informed consent was obtained from each patient. Genomic DNA samples were extracted from the peripheral blood using standard procedures. Clinically suspected vEDS patients were also analyzed by using the total RNA method (RT-PCR direct-sequencing) as described previously [5].

2.2. PCR for the hrMCA method

We designed 52 PCR primer pairs covering the entire coding region of COL3A1, containing 52 exons and the adjacent exon–intron junctions, by using the GenBank genetic sequence database (GenBank ID: NM_000090.3) as the reference (Supplementary Table 1). All primers were designed with the LightScanner Primer Design software program (Idaho Technology, UT, USA). The number of domains of each amplicon was predicted by Poland's algorithm (http://www.biophys.uni-duesseldorf.de/local/POLAND/poland.html) [14]. For each amplicon, the best annealing temperature for DNA amplification was determined by using a gradient temperature of 58 °C to 72 °C in a CFX96 Real-Time PCR detection system (Bio-Rad Laboratories, CA, USA) with control genomic DNA. DNA amplification was performed for each amplicon in 96-well microtiter plates with a 10-μl final volume containing 20 ng of genomic DNA, 200 μM each of deoxynucleotide triphosphates (dNTPs), 1× LCGreen Plus (Idaho Technology), 1× Ex Taq buffer, 0.5 U of Ex Taq enzyme (Takara Bio, Shiga, Japan), and 0.25 μM of each primer.

The thermocycling conditions were: 2 min at 95 °C, followed by 45 cycles of amplification consisting in 30 s at 94 °C and 30 s at gradient temperature from 62 °C to 67 °C. To promote heteroduplex formation, the samples were subsequently denatured by heating to 94 °C for 30 s and cooled to 25 °C for 30 s.

2.3. hrMCA

After the PCR, the plates were imaged in a 96-well LightScanner instrument (Idaho Technology) to examine the differences in the melting curves between the patient samples and the control. The plates were heated at 0.1 °C/s, and the fluorescence was measured from 70 °C to 98 °C. The melting curves were analyzed by using the LightScanner Call IT 1.5 software program (Idaho Technology) according to the manufacturer's protocol. All melting curves deviating from the wild-type curve and appearing as a different color in different plots potentially contain a variant.

2.4. Small amplicon genotyping (SAG) for coding-region SNPs (cSNPs) in COL3A1

We used a SAG method based on hrMCA to genotype three cSNPs with high frequency in COL3A1 [15,16]. These include rs1800255:G>A, rs1801184:T>C, and rs2271683:A>G on exons 31, 33, and 49 of COL3A1, respectively. All three primer pairs were set on each exon so that the same primer pairs could be used for both genomic DNA and cDNA to detect the sequence discrepancies between genomic DNA and cDNA of the same patient (Supplementary Table 2).

DNA amplification was performed in a 96-well plate with a 10-μl final volume containing 4 μl of 2.5× high-sensitivity genotyping master mix (Idaho Technology), 1 μM of each primer, and 20 ng of genomic DNA or cDNA derived from 25 ng of total RNA. The thermocycling conditions were: 2 min at 95 °C, followed by 45 cycles of 30 s at 94 °C and 30 s at 72.6 °C (rs1801184 and rs2271683) or 74.7 °C (rs1800255). After PCR, the plate was imaged in a LightScanner and genotype identification was performed manually by using internal calibration.

2.5. Cycle sequencing

Samples from vEDS patients showing abnormal hrMCA profiles were sequenced with BigDye Terminator v3 (Applied Biosystems, CA, USA) according to the manufacturer's protocol and analyzed with ABI Prism 3130 (Applied Biosystems).

3. Results

3.1. Primer design and PCR optimization for hrMCA of COL3A1

The optimized PCR primers for the entire coding region of COL3A1 are shown in Supplementary Table 1. The amplicon length was 124–330 bp, and the best annealing temperature was between 62 °C and 67 °C. There were 45 amplicons with two domains (which are a result of a high GC region with differences within the same amplicon) and seven amplicons with one domain. The expected number of domains by Poland's algorithm and the actual hrMCA-derived number of domains were almost the same (97% correct; data not shown). To maximize the sensitivity, the fragment of exon 49 was split into two amplicons.

3.2. COL3A1 mutation screening by hrMCA

After determining the best conditions, we set up a COL3A1 mutation screening system based on hrMCA using genomic DNA. In this system, three patient samples and one control could be simultaneously analyzed in three 96-well plates (data not shown). When we started to check the differences in the melting curves between the patient samples and control by hrMCA, we obtained false positive different melting curves with the same nucleotide sequences in the same amplicon. These samples showed a large difference in Ct values, a fractional number of cycles in the PCR amplification curve of the real-time PCR, in the same amplicon detected by the real-time PCR detection instrument. The Ct value should be the same for each amplicon when the same primers are used to assay the mutant target [17]. In this study, the Ct value of each amplicon was 23–33 (mean = 25) (data not shown). Therefore, we used of all the samples with the same Ct value (Ct ± 0.7) within the same amplicon to reduce the false positives.

In eight validation samples, all mutations were correctly identified (Table 1A), including five missense (Fig. 1A–D) and three splice-site (Fig. 1H and I) mutations. Next, among clinically suspected vEDS patients, we found COL3A1 mutations in seven patients, including five novel mutations, by the hrMCA method followed by sequencing (Table 1B). The mutations included two novel missense mutations (c.539G>A; Fig. 1E, and c.2150G>A; Fig. 1F), three splice-site mutations (one novel splice-mutation at c.897+1G>C; Fig. 1G and two at c.1662+1G>A; Fig. 1I), one novel nonsense mutation (c.2992C>T; Fig. 1J) and one novel deletion mutation (1-bp) in exon 32 (c.2187delA; Fig. 1K). We also evaluated six of the seven suspected clinical samples by the total RNA method, but the nonsense mutation found by the hrMCA in genomic DNA could not be detected by the total RNA method. The deletion mutation (c.2187delA) had a frameshift, leading to a

Table 1
COL3A1 mutations detected by hrMCA of genomic DNA.

Mutation type (s)	Location	Variation	Effect	Nucleotide patterns (Wild/Mutant)	Index	Reference	Fig. 1
A. Validation samples							
Missense	Exon 18	c.1159G>T	p.G387 W	G/T	1	[5]	A
Missense	Exon 27	c.1844G>A	p.G615E	G/A	1	[5]	B
Missense	Exon 42	c.2995G>A	p.G999S	G/A	1	[4]	C
Missense	Exon 44	c.3131G>A	p.G1044D	G/A	2	[18]	D
Splice-site	Intron 20	c.1347+1 G>A		G/A	1	[5]	H
Splice-site	Intron 24	c.1662+1G>A		G/A	3[a]	[19]	I
Splice-site	Intron 24	c.1662+2 T>G		T/G	1	[20]	I

Mutation type (s)	Location	Variation	Effect	Nucleotide patterns (Wild/Mutant)	Index	Fig. 1
B. Novel mutations						
Missense	Exon 7	c.539G>A	p.G180D	G/A	1	E
Missense	Exon 32	c.2150G>A	p.G717D	G/A	1	F
Splice-site	Intron 13	c.897+1G>C		G/C	1	G
Nonsense	Exon 42	c.2992C>T	p.Q998X	C/T	1	J
Frameshift (deletion)	Exon 32	c.2187delA		A/del	1	K

Coding (c.) and protein (p.) sequences of COL3A1 are shown by the GenBank ID: NM_000090.3 with +1 corresponding to A of the ATG initiation codon.
 [a] One sample was a validation sample and two were clinically suspected vEDS samples.
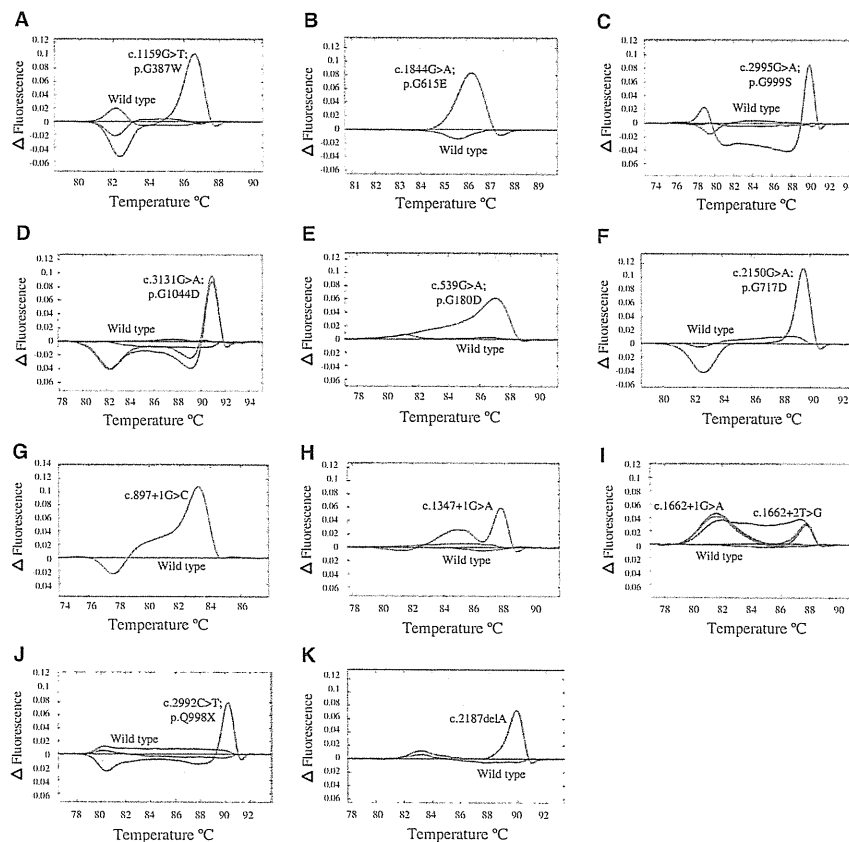

Fig. 1. Different types of COL3A1 mutations detection by the hrMCA method: missense mutations (A–F), splice-site mutations (G–I), mutations with nonsense-mediated mRNA decay; nonsense (J) and 1 bp deletion (K). Different melting curve patterns are shown between wild type and mutant COL3A1. (A) c.1159G>T in exon 18; (B) c.1844G>A in exon 27; (C) c.2995G>A in exon 42; (D) c.3131G>A in exon 44 (two different individuals); (E) c.539G>A in exon 7; (F) c.2150G>A in exon 32; (G) c.897+1G>C at intron 13; (H) c.1347+1G>A at intron 20; (I) c.1662+1G>A (three different individuals), and c.1662+2T>G (one individual) at intron 24; (J) c.2992C>T in exon 42; (K) c.2187delA in exon 32.

premature termination codon (TAG) 181 nucleotides downstream in exon 35.

Two samples from different individuals with the same mutation at c.3131G>A in exon 44 showed the same melting curve pattern (Fig. 1D). In exon 24 amplicon, four splice-site mutations (three c.1662+1G>A from different individuals and one c.1662+2T>G; Fig. 1I) were analyzed together by the hrMCA method. The three samples with the c.1662+1G>A mutation showed the same pattern, but the c.1662+2T>G sample showed a different pattern; all

melting curves were different from the control. These results showed the high sensitivity and specificity of the hrMCA method.

3.3. Heterozygous cSNPs screening by SAG

The hrMCA method could not distinguish between mutations and SNPs. Among 12 Japanese patients, we found 9 samples with one of three common cSNPs of COL3A1 (rs1800255:G>A, rs1801184:T>C, and rs2271683:A>G) by sequencing. One of these

cSNPs is present in more than half of the European or Japanese population (http://www.ncbi.nlm.nih.gov/snp/). Therefore, to predict the common heterozygous cSNPs in COL3A1 by the SAG method is important to reduce unnecessary sequencing. By the SAG method (Supplementary Table 2), both genomic DNA and cDNA from the same patient showed the same reproducible pattern for all three cSNPs (Fig. 2A–C), and we could clearly differentiate between the wild type (homozygous) and the SNP type (heterozygous) for all three cSNPs.

When this SAG method was applied for the patient with the nonsense mutation, the results showed different melting curves between genomic DNA and cDNA at two heterozygous cSNPs (rs1801184:T>C, and rs2271683:A>G) (Fig. 2D and E), suggesting that there were nucleotide discrepancies between genomic DNA and cDNA of the same patient. In this sample, we also found sequence discrepancies between genomic DNA and cDNA at the two heterozygous cSNPs and the nonsense mutation position (c.2992C>T) by sequencing (data not shown).

4. Discussion

We successfully established a method for mutation screening of the entire coding region of COL3A1 for diagnosis of vEDS using gradient PCR reactions and the hrMCA method for genomic DNA, followed by sequencing of abnormal hrMCA exons. By this method, COL3A1 mutations can be screened easily and rapidly with high sensitivity and specificity without an invasive skin biopsy procedure. In addition, this system enables to detect more COL3A1 mutations caused by nonsense-mediated mRNA decay (NMD), nonsense mutations and small deletions that could not be detected by the conventional total RNA method.

For screening COL3A1 mutations, two important factors were noted that indicate the superiority of the hrMCA method. First, COL3A1 mutations are heterozygous in an autosomal dominant manner, which favors higher sensitivity and specificity in hrMCA than those for homozygous mutations [21,22]. The heterozygous detection rate has nearly 100% sensitivity [23], because heterozygotes form a proportion of heteroduplexes which melt differently to perfectly matched homoduplexes [24]. Second, the nucleotide levels in COL3A1 mutations are preferable for hrMCA because a higher difference in the melting temperature results in a greater difference between the mutant melting curve and the control as

determined by the hrMCA method [15]. The mutation patterns of G/A or T/C and G/T or A/C had a melting temperature that differed by 2 °C from the control, whereas the G/C or A/T patterns had only a 1 °C difference [12,15]. According to the reported COL3A1 mutations, more than 85% of the missense and splice-site mutations showed G/A or G/T or T/C patterns (Human Gene Mutation Database (HGMD; http://www.hgmd.cf.ac.uk/ac/all.php)), which can be easily detected by the hrMCA method because of the greater melting temperature difference between the mutant and the wild type.

In determining the hrMCA conditions for the primer setting in each exon, the number of melting domains, which are a result of a high GC difference within the amplicon, should be considered. The number of domains for each amplicon could be predicted by Poland's algorithm before making the primers. Because hrMCA depends on the GC content of the amplicon, multiple domains can mask the presence of a mutation. Some researchers argue strongly for the use of small products, and against the use of multiple domains [25,26], but the optimal number of domains for hrMCA is still unclear [22]. In our experiment, we were able to generate the amplicon with shortest possible length in each exon containing one or two melting domains because the length of each exon of COL3A1 is short.

It is important to reduce the false-positive results obtained by hrMCA. Samples with insufficient amplification should be reanalyzed from the PCR step in hrMCA [14]. However, it is sometimes difficult to determine whether amplification is sufficient. Therefore, we used the same Ct value (Ct ± 0.7) as a standard which is easy to evaluate, and the number of false-positive samples was reduced. For amplification of hrMCA samples, it is important to select the samples that have the same Ct value in each amplicon using a real-time PCR detection system.

In the present study, a nonsense mutation (c.2992C>T) could be detected only from genomic DNA by the hrMCA method, but not by the total RNA method. This discrepancy between genomic DNA and cDNA occurs because mRNA of the mutant allele does not mature as a result of NMD [27]. The deletion mutation (c.2187delA) in this study leads to a frameshift, causing a premature termination codon in exon 35 and is predicted not to be detected by the conventional total RNA method because of NMD [27,28]. In COL3A1, the reported mutations with NMD are very rare compared to other collagen gene mutations that cause diseases, because most COL3A1 mutations have been detected previously using the total RNA method. The hrMCA method using genomic DNA in this study showed
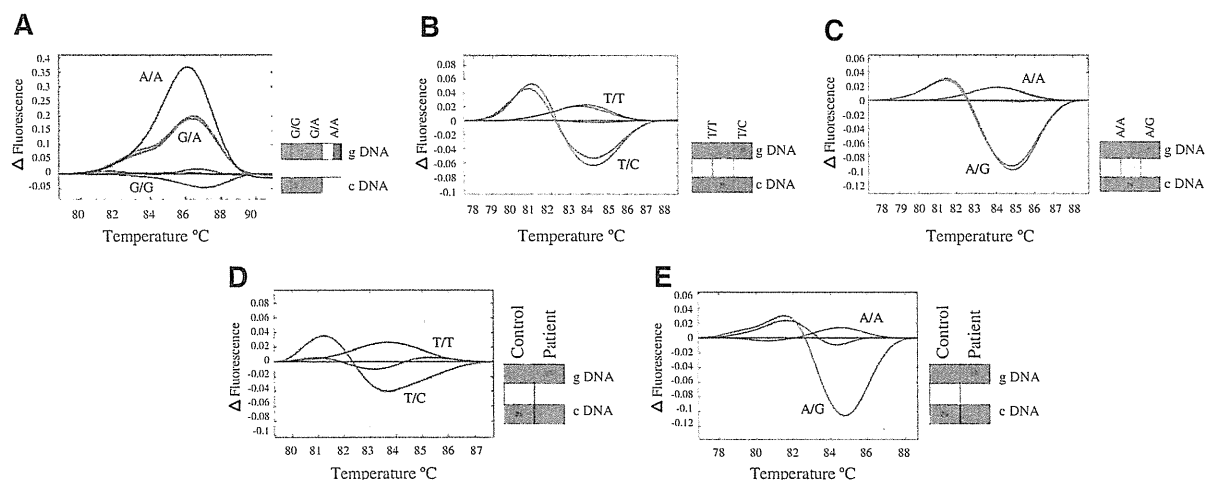

Fig. 2. COL3A1 cSNP detection by the SAG method using genomic DNA and cDNA from the same individual: (A–C) Different melting curve patterns are shown between wild-type (homozygous) and SNP-type (heterozygous) in three common cSNPs. (A) rs1800255:G>A in exon 31 (G/G, G/A, A/A); (B) rs1801184:T>C in exon 33 (T/T, T/C); (C) rs2271683:A>G in exon 49 (A/A, A/G) genotypes. (D and E) Melting curve discrepancies between genomic DNA and cDNA are shown in COL3A1 nonsense mutation patient compared to the control. (D) rs1801184:T>C in exon 33 and (E) rs2271683:A>G in exon 49.

higher mutation detection efficiency than the total RNA method. The number of mutations in COL3A1, including those caused by NMD, will likely be increased by mutation screening using genomic DNA. Screening of COL3A1 mutations should be performed for the entire coding region of the gene by using genomic DNA for all patients showing the typical features of vEDS, regardless of whether there are negative findings based on a cDNA analysis, because nonsense mutations can occur at any position in the coding region.

Our SAG method enabled screening of the three most common cSNPs with high frequencies in COL3A1, and for prediction of cSNPs or mutations before sequencing. By the SAG method, nonsense mutations with any of the heterogeneous cSNPs of COL3A1 can be predicted by checking for discrepancies between genomic DNA and cDNA. Therefore, our establishment of hrMCA for exon screening in combination with SAG of cSNPs from genomic DNA enables detection of COL3A1 mutations with high sensitivity and specificity using a minimally-invasive procedure.

Emphasizing the importance of the new screening method, NMD has been shown to modulate the clinical outcome of genetic diseases [29]. In COL3A1, the phenotype severities might differ between different types of COL3A1 mutations [28]. In the case of missense and splice-site mutations, production of the COL3A1 protein is reduced to one-eighth of the usual amount because of a dominant negative effect [2]. However, in the case of mutations with NMD, such as frame shift and nonsense mutations, the production of COL3A1 is reduced by half because of haploinsufficiency. Approaches to protect transcripts containing a premature termination codon from NMD could potentially be used as an alternative treatment [29]. A better understanding of the genotype–phenotype correlation in COL3A1 using this method will lead to improve in the diagnosis and treatment of vEDS.

Acknowledgments

Appendix A. Supplementary data

Supplementary data associated with this article can be found, in the online version, at doi:10.1016/j.bbrc.2011.01.011.

References

[1] D.P. Germain, Ehlers-Danlos syndrome type IV, Orphanet J. Rare Dis. 2 (2007) 32.
[2] A. Watanabe, T. Shimada, Vascular type of Ehlers-Danlos syndrome, J. Nippon Med. Sch. 75 (2008) 254–261.
[3] R. Dalgleish, The human collagen mutation database 1998, Nucl. Acids Res. 26 (1998) 253–255.
[4] M. Pepin, U. Schwarze, A. Superti-Furga, P.H. Byers, Clinical and genetic features of Ehlers-Danlos syndrome type IV, the vascular type, N. Engl. J. Med. 342 (2000) 673–680.
[5] A. Watanabe, T. Kosho, T. Wada, N. Sakai, M. Fujimoto, Y. Fukushima, T. Shimada, Genetic aspects of the vascular type of Ehlers-Danlos syndrome (vEDS, EDSIV) in Japan, Circ. J. 71 (2007) 261–265.
[6] B.L. Loeys, U. Schwarze, T. Holm, B.L. Callewaert, G.H. Thomas, H. Pannu, J.F. De Backer, G.L. Oswald, S. Symoens, S. Manouvrier, A.E. Roberts, F. Faravelli, M.A. Greco, R.E. Pyeritz, D.M. Milewicz, P.J. Coucke, D.E. Cameron, A.C. Braverman, P.H. Byers, A.M. De Paepe, H.C. Dietz, Aneurysm syndromes caused by mutations in the TGF-beta receptor, N. Engl. J. Med. 355 (2006) 788–798.
[7] M. Orita, H. Iwahana, H. Kanazawa, K. Hayashi, T. Sekiya, Detection of polymorphisms of human DNA by gel electrophoresis as single-strand conformation polymorphisms, Proc. Natl Acad. Sci. USA 86 (1989) 2766–2770.
[8] E. Holinski-Feder, Y. Muller-Koch, W. Friedl, G. Moeslein, G. Keller, J. Plaschke, W. Ballhausen, M. Gross, K. Baldwin-Jedele, M. Jungck, E. Mangold, H. Vogelsang, H.K. Schackert, P. Lohsea, J. Murken, T. Meitinger, DHPLC mutation analysis of the hereditary nonpolyposis colon cancer (HNPCC) genes hMLH1 and hMSH2, J. Biochem. Biophys. Methods 47 (2001) 21–32.
[9] C.T. Wittwer, G.H. Reed, C.N. Gundry, J.G. Vandersteen, R.J. Pryor, High-resolution genotyping by amplicon melting analysis using LCGreen, Clin. Chem. 49 (2003) 853–860.
[10] N. van der Stoep, C.D. van Paridon, T. Janssens, P. Krenkova, A. Stambergova, M. Macek, G. Matthijs, E. Bakker, Diagnostic guidelines for high-resolution melting curve (HRM) analysis: an interlaboratory validation of BRCA1 mutation scanning using the 96-well LightScanner, Hum. Mutat. 30 (2009) 899–909.
[11] E. Rouleau, C. Lefol, V. Bourdon, F. Coulet, T. Noguchi, F. Soubrier, I. Bieche, S. Olschwang, H. Sobol, R. Lidereau, Quantitative PCR high-resolution melting (qPCR-HRM) curve analysis, a new approach to simultaneously screen point mutations and large rearrangements: application to MLH1 germline mutations in Lynch syndrome, Hum. Mutat. 30 (2009) 867–875.
[12] G.H. Reed, C.T. Wittwer, Sensitivity and specificity of single-nucleotide polymorphism scanning by high-resolution melting analysis, Clin. Chem. 50 (2004) 1748–1754.
[13] R. Almomani, N. van der Stoep, E. Bakker, J.T. den Dunnen, M.H. Breuning, I.B. Ginjaar, Rapid and cost effective detection of small mutations in the DMD gene by high resolution melting curve analysis, Neuromuscul. Disord. 19 (2009) 383–390.
[14] H. Do, M. Krypuy, P.L. Mitchell, S.B. Fox, A. Dobrovic, High resolution melting analysis for rapid and sensitive EGFR and KRAS mutation detection in formalin fixed paraffin embedded biopsies, BMC Cancer 8 (2008) 142.
[15] M. Liew, R. Pryor, R. Palais, C. Meadows, M. Erali, E. Lyon, C. Wittwer, Genotyping of single-nucleotide polymorphisms by high-resolution melting of small amplicons, Clin. Chem. 50 (2004) 1156–1164.
[16] J. Montgomery, C.T. Wittwer, R. Palais, L. Zhou, Simultaneous mutation scanning and genotyping by high-resolution DNA melting analysis, Nat. Protoc. 2 (2007) 59–66.
[17] J. Morlan, J. Baker, D. Sinicropi, Mutation detection by real-time PCR: a simple, robust and highly selective method, PLoS One 4 (2009) e4584.
[18] Y. Nishiyama, J. Nejima, A. Watanabe, E. Kotani, N. Sakai, A. Hatamochi, H. Shinkai, K. Kiuchi, K. Tamura, T. Shimada, T. Takano, Y. Katayama, Ehlers-Danlos syndrome type IV with a unique point mutation in COL3A1 and familial phenotype of myocardial infarction without organic coronary stenosis, J. Intern. Med. 249 (2001) 103–108.
[19] U. Schwarze, J.A. Goldstein, P.H. Byers, Splicing defects in the COL3A1 gene: marked preference for 5' (donor) spice-site mutations in patients with exon-skipping mutations and Ehlers-Danlos syndrome type IV, Am. J. Hum. Genet. 61 (1997) 1276–1286.
[20] O. Okamoto, T. Ando, A. Watanabe, F. Sato, H. Mimata, T. Shimada, S. Fujiwara, A novel point mutation in type III collagen gene resulting in exon 24 skipping in a case of vascular type Ehlers-Danlos syndrome, Arch. Dermatol. Res. 300 (2008) 525–529.
[21] R.H. Vossen, E. Aten, A. Roos, J.T. den Dunnen, High-resolution melting analysis (HRMA): more than just sequence variant screening, Hum. Mutat. 30 (2009) 860–866.
[22] C.T. Wittwer, High-resolution DNA melting analysis: advancements and limitations, Hum. Mutat. 30 (2009) 857–859.
[23] L.S. Chou, E. Lyon, C.T. Wittwer, A comparison of high-resolution melting analysis with denaturing high-performance liquid chromatography for mutation scanning: cystic fibrosis transmembrane conductance regulator gene as a model, Am. J. Clin. Pathol. 124 (2005) 330–338.
[24] E.A. Takano, G. Mitchell, S.B. Fox, A. Dobrovic, Rapid detection of carriers with BRCA1 and BRCA2 mutations using high resolution melting analysis, BMC Cancer 8 (2008) 59.
[25] E.A. Tindall, D.C. Petersen, P. Woodbridge, K. Schipany, V.M. Hayes, Assessing high-resolution melt curve analysis for accurate detection of gene variants in complex DNA fragments, Hum. Mutat. 30 (2009) 876–883.
[26] M. Krypuy, A.A. Ahmed, D. Etemadmoghadam, S.J. Hyland, A. DeFazio, S.B. Fox, J.D. Brenton, D.D. Bowtell, A. Dobrovic, High resolution melting for mutation scanning of TP53 exons 5–8, BMC Cancer 7 (2007) 168.
[27] U. Schwarze, W.I. Schievink, E. Petty, M.R. Jaff, D. Babovic-Vuksanovic, K.J. Cherry, M. Pepin, P.H. Byers, Haploinsufficiency for one COL3A1 allele of type III procollagen results in a phenotype similar to the vascular form of Ehlers-Danlos syndrome, Ehlers-Danlos syndrome type IV, Am. J. Hum. Genet. 69 (2001) 989–1001.
[28] A. Plancke, M. Holder-Espinasse, V. Rigau, S. Manouvrier, M. Claustres, P. Khau Van Kien, Homozygosity for a null allele of COL3A1 results in recessive Ehlers-Danlos syndrome, Eur. J. Hum. Genet. 17 (2009) 1411–1416.
[29] M. Khajavi, K. Inoue, J.R. Lupski, Nonsense-mediated mRNA decay modulates clinical outcome of genetic disease, Eur. J. Hum. Genet. 14 (2006) 1074–1081.